Available online at www.sciencedirect.com
SCIENCE DIRECT
Biochemical Pharmacology 70 (2005) 770–785
Biochemical Pharmacology
www.elsevier.com/locate/biochempharm

# Presence of diverse functional P2X receptors in rat cerebellar synaptic terminals

Cristina Hervás, Raquel Pérez-Sen, M Teresa Miras-Portugal *

*Department of Biochemistry, Veterinary Faculty, Universidad Complutense de Madrid, Avda. Puerta de Hierro s/n, 28040 Madrid, Spain*

Received 18 March 2005; accepted 18 May 2005

**Abstract**

Studies in individual synaptic terminals have demonstrated the presence of diverse functional P2X receptors in rat cerebellum. No immunolabelling for $P2X_1$, $P2X_4$, $P2X_5$ and $P2X_6$, and scarce presence of $P2X_2$ were found at the cerebellar synaptic terminals. $P2X_3$ immunolabelling was present in 28% of isolated synaptosomes. At these synaptic terminals, nucleotides as ATP or α,β-meATP induced $Ca^{2+}$ transients in the presence of extracellular $Ca^{2+}$, showing homologous and heterologous receptor desensitization in 60% of cases. $Ip_5I$ 10 nM did not block responses to α,β-meATP, but inhibition occurred when antagonist concentrations were equal or higher than 100 nM. These data agree with the presence of abundant $P2X_3$ homomeric receptors. $P2X_7$ immunolabelling was present in 60% of terminals and $P2X_7$ receptor hallmarks in $Ca^{2+}$ responses have been found. BzATP was more potent than ATP and responses were potentiated when assayed in $Mg^{2+}$-free medium. $EC_{50}$ values were, respectively, $39.4 \pm 0.4$ and $0.3 \pm 0.1$ μM for ATP in the presence or absence of $Mg^{2+}$. Maximal values of synaptosomal calcium transients, in the presence or absence of $Mg^{2+}$, were, respectively, $91.6 \pm 11.9$ and $132.9 \pm 12.9$ nM for ATP; and $104.3 \pm 9.4$ and $169.7 \pm 17.1$ nM for BzATP. In addition, $Zn^{2+}$ inhibited ATP responses in the absence of $Mg^{2+}$ and the $P2X_7$ specific antagonist Brilliant Blue G completely blocked these responses in one half of synaptosomes. This study reports the presence of functional $P2X_3$ and $P2X_7$ receptors at synaptic sites, which provides complexity and regulatory possibilities to the cerebellar neurotransmission.


## 1. Introduction

The role of ATP as a neurotransmitter in both the peripheral and central nervous system (CNS) is widely accepted. Extracellular functions of ATP are mediated through a family of receptors, known as P2, which are divided into two subclasses: metabotropic G-protein-coupled receptors (P2Y) and ionotropic receptors (P2X) [1]. Seven different P2X subunits ($P2X_{1-7}$) from mammalian species have been identified [2,3]. They assemble to form functional homomultimeric or heteromultimeric receptors as demostrated by cDNA expression assays and pharmacological properties of native receptors [4,5].

ATP and other nucleotides are released after synaptic terminal stimulation, and once at extracellular medium, they can activate different nucleotide receptors [6–8]. Pintor and Miras-Portugal [9] showed that synaptic terminals isolated from rat midbrain respond to ATP, and also diadenosine polyphosphates, by increasing the intrasynaptosomal calcium concentration. This was the first demonstration of the presence of independent pre-synaptic ionotropic receptors for nucleotides and dinucleotides in the CNS. In this model, the effect of ATP appeared to be mediated by a P2X receptor, which showed $P2X_2$ and $P2X_3$ pharmacological properties [10,11]. Recently, evidences of functional $P2X_7$ receptors expressed in midbrain synaptosomes have also been reported [12], contributing with new data to several reports that attribute a role to pre-synaptic $P2X_7$ receptors in the CNS. Although this subunit was cloned at first from brain, no function appeared to be appointed to $P2X_7$ receptors in neurons, and it was reported to be mainly restricted to cells involved in immune functions. Nowadays, these receptors have been already described at many neural locations, such as synaptic excitatory terminals in the medulla oblongata, spinal cord, neuromuscular junction, hippocampus or cortex [13–16].

In the last few years, it has been demonstrated that activation of pre-synaptic P2X receptors can modulate glutamate, norepinephrine, glycine, acetylcholine and

* Corresponding author. Tel.: +34 1 394 38 94; fax: +34 1 394 39 09.
*E-mail address:* mtmiras@vet.ucm.es (M.T. Miras-Portugal).

0006-2952/$ – see front matter © 2005 Elsevier Inc. All rights reserved.
doi:10.1016/j.bcp.2005.05.033

GABA release, that might consequently modify synaptic efficiency in the CNS, pointing to a regulatory role of P2X receptors in synaptic neurotransmission [17–21]. Concerning specifically the $P2X_7$ receptors, their activation promotes vesicular release at neuromuscular junction and in a similar extent glutamate release in the CNS [13,22]. This is the case of excitatory hippocampal neurons where $P2X_7$ receptors activation evokes glutamate release that subsequently modulates GABA release from nearby neurons [15]. A recent work has suggested pre-synaptic mechanisms, such as modulation of action potential width or an increase in pre-synaptic terminal excitability, underlying the enhancement of evoked transmitter release by $P2X_7$ receptors activation [23]. In an opposite way, $P2X_7$ receptors mediate depression of synaptic transmission in the CA3 region of the hippocampus [14], suggesting diverse roles of $P2X_7$ receptors in synaptic transmission.

Cerebellar structures exhibit high levels of P2X subunits expression [3]. In cultured granule neurons from rat cerebellum, the presence of $P2X_1$, $P2X_2$, $P2X_3$, $P2X_4$, $P2X_6$ and $P2X_7$, has been confirmed by RT-PCR. In addition, in cultured Purkinje and granule cells, the activation of P2X receptors results in calcium transients, dependent on the presence of extracellular calcium [24–26]. It is noteworthy the high density of $P2X_3$ subunits in a punctate distribution, revealed by immunohistochemical data at the cellular fibers of cerebellar granule cells, where they co-localize with the synaptic vesicle marker synaptophysin, and those of $P2X_1$ in a more continuous way along the neural fibers. Concerning the $P2X_7$ subunit immunolabelling, recent reports point to the labelling of other related proteins, in addition to this subunit [27].

The aim of this work has been to study the presence and functional properties of P2X receptors in pre-synaptic terminals of rat cerebellum. Immunocytochemical and microfluorimetric techniques have been employed to characterize the P2X diversity in synaptic terminals isolated from adult rat cerebellum. Results here reported confirm that widespread distribution of functional P2X receptors exists in cerebellum, throughout the synaptic sites. These receptors respond with calcium transients to ATP and other more specific analogs of the diverse subtypes, thus pointing to an important role of P2X receptors in cerebellar neurotransmission at the pre-synaptic level.

## 2. Methods

### 2.1. Synaptosomal preparation and granule cell culture

Synaptosomes were obtained from the rat cerebellum of adult male Wistar rats (6–7 weeks old). The isolation procedure was the same for synaptosomes used in immunochemical and calcium microfluorimetric assays, both purified using a Percoll gradient as described by Dunkley et al. [28].

Primary cultures of cerebellar granule cells (CGC) were obtained from 7-day-old Wistar rats as previously described [25]. CGC were seeded at a density of $10^5$ cells/cm$^2$ on poly-lysine coated glass coverslips and grown in Neurobasal A medium (Gibco, NY, USA) containing 2% B27 supplement (Gibco), 20 mM KCl, 2 mM glutamine (Sigma, St. Louis, MO, USA), 100 U/mL penicillin, 0.1 mg/mL streptomycin and 0.25 μg/mL amphoterycin (Biochrom AG, Berlin, Germany) in a humidified atmosphere of 5% $CO_2$ at 37 °C.

All the experiments carried out at the Universidad Complutense of Madrid were performed according to the guidelines of the International Council for Laboratory Animal Science (ICLAS).

### 2.2. $Ca^{2+}$ measurements in single synaptosomes

Synaptosomal pellets containing 0.5 mg of protein, obtained by means of a Percoll gradient, were re-suspended in 1 mL hypertonic buffered medium (HBM), composition (in mM): NaCl, 140; KCl, 5; $NaHCO_3$, 5; $NaH_2PO_4$, 1.2; $MgCl_2$, 1; glucose, 10; HEPES 10; pH 7.4; and loaded with 5 μM Fura-2 AM (Molecular Probes, Eugene, OR) for 45 min at 37 °C. After loading, synaptosomes were placed on coverslips coated with poly-L-lysine for 45 min at room temperature. This time period is sufficient for sticking to the substrate. Next, the coverslips were washed with fresh HBM containing 1.33 mM $CaCl_2$ and mounted in a small superfusion chamber on the stage of a NIKON-TE 200 microscope. The volume of the chamber accounts for 34 μL and the perfusion speed was 1.5 mL/min. The synaptosomes were then superfused continuously with HBM medium. Agonists were applied during 30 s and a pulse of 30 mM KCl was applied at the end of each experiment to confirm the functionality and viability of the synaptosomes under study. Time course between different applications was at least 1 min. For the experiments carried out in the absence of $Mg^{2+}$ ions, the agonist was diluted in HBM medium in which magnesium had been replaced by the correspondent concentration of glucose, as also in the superfusion media. When antagonists were assayed, they were applied 2 min before and kept during agonist stimulation [9,11].

Synaptosomes were imaged through a NIKON TE-200 microscope 100× lens (S Fluor 0.5–1.3 oil iris). Emitted light was isolated by a dichroic mirror (430 nm) and a 510 nm band pass filter (Omega Optical). The wavelength of the incoming light was selected with the aid of a monochromator (12 nm bandwidth, Perkin-Elmer Life Sciences, Cambridge, UK) set at 340 and 380 nm. These wavelengths correspond to the fluorescence peaks of $Ca^{2+}$-saturated and $Ca^{2+}$-free Fura-2 solutions. Twelve bit images were obtained using an Ultrapix 2000 Mono CCD camera controlled by Ultraview PC software

(Perkin-Elmer Life Sciences, Cambridge, UK) (Fig. 6B). The exposure time was 50 ms and wavelength change over time <5 ms. Time course data represent the average light intensity in a small circle (0.5–1.5 μm diameter). Background and autofluorescence components were subtracted at each wavelength and the ratio 340/380 was calibrated into $[Ca^{2+}]_i$ values using the Grynkyevicz's equation [29]. The variables $R_{max}$, $R_{min}$ and $\beta$ were calculated "in vitro" from the spectra of small Fura-2 droplets in $Ca^{2+}$-saturated solution (composition mM: KCl, 100; NaCl, 10; $MgCl_2$, 1; 4-morpholinepropanesulfonic acid (MOPS), 10; $CaCl_2$, 2.5; Fura-2 acid, 0.01) and $Ca^{2+}$-free solution (composition mM: KCl 100, NaCl 10, $MgCl_2$ 1, MOPS 10, Fura-2 acid 0.01 and EGTA 5), both determined empirically in our system [11].

Adenosine 5′ triphosphate (ATP), alpha,beta-methylene ATP (α,β-meATP), 2′-3′-*O*-(4-benzoylbenzoyl)-adenosine 5′-triphosphate (BzATP) and Brilliant Blue G used in microfluorimetric studies, were all obtained from Sigma Chemicals. Diinosine pentaphosphate ($Ip_5I$) was synthesized as indicated in a previous work [30].

### 2.3. Immunocytochemical assays

For the immunofluorescence assays, the coverslips containing glued synaptosomes or cultured granule cells were fixed with 4% paraformaldehyde (PFA) (Sigma) (w/v) for 15 min, washed twice in phosphate-buffered saline (PBS) and incubated for 1 h in PBS containing 3% bovine serum albumin (BSA) (Sigma) (w/v), 0.1% Triton X-100 (v/v) and 5% normal goat serum (Sigma) (v/v). The preparations were washed twice and incubated with the primary antibody for 1 h at 37 °C. Primary antibodies were diluted in PBS/BSA, and recognized the specified rat proteins: mouse anti-synaptophysin (1:200) (Sigma), rabbit anti-vesicular glutamate transporter 1 (VGLUT1) (1:1000) (Synaptic Systems, Goettingen, Germany), rabbit anti-vesicular glutamate transporter 2 (VGLUT2) (1:500) (Synaptic Systems), mouse anti-glutamic acid decarboxylase (GAD) (5 μg/mL; Boehringer Mannheim); rabbit anti-$P2X_1$, $P2X_7$ (1:100) and guinea-pig anti-$P2X_2$, $P2X_3$ (1:100) (Chemicon), rabbit anti-$P2X_4$ (1:100) (Alomone Labs, Jerusalem), rabbit anti-$P2X_5$ (1:500) (a gift from M. Voigt) and rabbit anti-$P2X_6$ (1:500) (a gift from F. Soto). The coverslips were then washed three times and incubated for 1 h at 37 °C with the appropriate secondary antibodies: goat anti-mouse IgG fluorescein isothiocyanate-conjugated (FITC) (1:500) (Sigma), goat anti-rabbit IgG tetramethylrhodamine isothiocyanate-conjugated (TRICT) (Sigma) (1:500) and goat anti-guinea pig IgG rhodamine-conjugated (TRICT) (1:500). Finally, preparations were washed three times and mounted following standard procedures. Control preparations were made according to the same protocol, but primary antibodies were replaced by the same volume of PBS/BSA solution.

The coverslips were viewed with a NIKON TE-200 microscope and a Kappa DX2 camera controlled by Kappa Image Base Control software. Images were afterwards analysed with Lucida 3.0 software (Kinetic Imaging, Nottingham, UK) to subtract no-especific fluorescence and Paint Shop Pro (Jasc Software) to obtain merged images.

### 2.4. Western blotting

Western blot experiments were performed using synaptosomal proteins extracted from cerebellar membranes, as previously described [31]. Membranes were incubated overnight at 4 °C with an antibody that recognizes $P2X_7$ receptor from Chemicon (Temecula, CA, USA) at 1:500 dilutions. As secondary antibody, incubated 1 h at room temperature, we used anti-rabbit IgG peroxidase linked (Amersham Bioscience) at 1:5000.

## 3. Results

### 3.1. Immunochemical characterization of rat cerebellar synaptic terminals

Rat cerebellar synaptosomes were obtained as described under Section 2 and labelled with an anti-synaptophysin antibody, a specific marker of synaptic vesicles that allows identify the total amount of pre-synaptic terminals in our preparation (Fig. 1A and D). The presence of glutamatergic terminals was detected with an antibody raised against the specific vesicular glutamate transporters VGLUT1 and VGLUT2. This preparation shows a high density of labelling with the antibody directed to VGLUT1 (Fig. 1B), which represents 52 ± 2% ($n = 3$) of the total labelled with synaptophysin (Fig. 1C). The vesicular glutamate transporter VGLUT2 was found in a lower percentage, accounting for 13 ± 2% ($n = 3$) of terminals labelled with synaptophysin (Fig. 1D–F).

The presence of GABAergic terminals in rat cerebellar synaptosomal preparations was detected with an antibody directed against the neural isoform of GAD, the key enzyme in the biosynthesis of GABA. These terminals account for 34% of the total labelled with synaptophysin ($n = 3$). As it is shown in Fig. 1G–I, there is no co-localization between terminals marked with VGLUT1 and those labelled with GAD, thus supporting the independent existence of excitatory and inhibitory synaptosomes in cerebellar preparations.

The great abundance of granule cells in cerebellum, which are glutamatergic, well correlates with the high number of terminals exhibiting positive labelling to VGLUT1 and VGLUT2. In a similar way, although in a lower extent, the presence of GABAergic terminals correlates with Purkinje, and also, stellate, basquet and Golgi neurons in cerebellar structures.

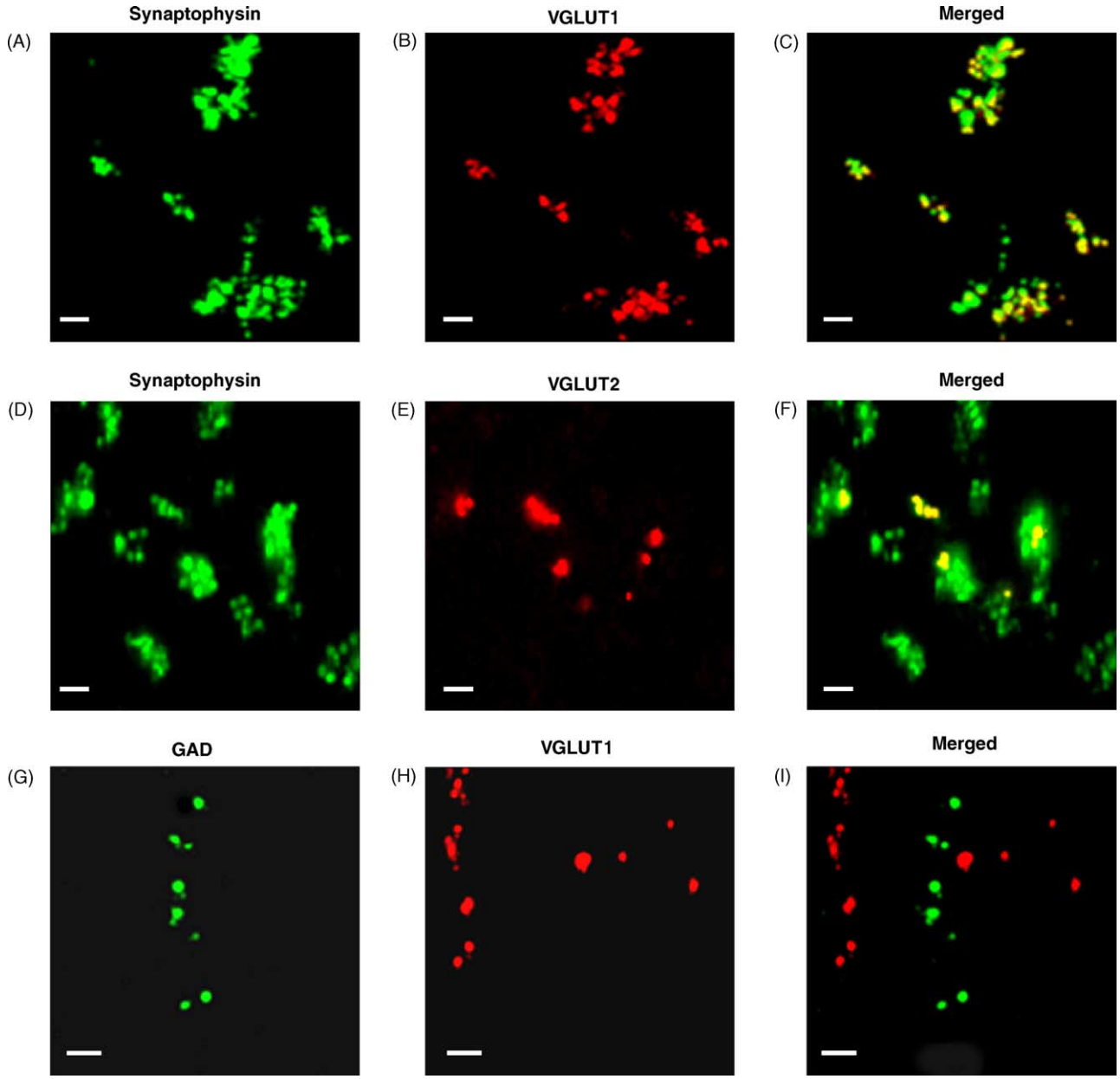


Fig. 1. Immunochemical characterization of glutamatergic and GABAergic terminals in rat cerebellar synaptosomal preparations. (A–F) Co-localization of VGLUT1 transporters with synaptophysin. Rat cerebellar synaptic terminals were labelled with mouse anti-synaptophysin antibodies and either rabbit anti-VGLUT1 or rabbit anti-VGLUT2 antibodies. Secondary visualization systems were (FITC)-coupled goat anti-mouse IgG and (TRICT)-conjugated goat anti-rabbit IgG. FITC- and TRICT-fluorescence images were sequentially collected, as described in Section 2. (A and D) Fluorescence image shows anti-synaptophysin-FITC immunolabelling; (B and E) respectively, same fields as (A and D), viewed in rhodamine optics reveals anti-VGLUT1 or anti-VGLUT2-TRICT immunostaining. (C and F) Images of (A and B) or (D and E) are overlaid showing co-localization of synaptophysin/VGLUT1 or synaptophysin/VGLUT2. (G–I) Negative co-localization of GAD and VGLUT1. (G) Fluorescence image shows anti-GAD-FITC immunolabelling. (H) Same field viewed with rhodamine optics reveals anti-VGLUT1-TRICT immunostaining. (I) Merge of anti-GAD and anti-VGLUT1 staining is shown. Scale bars = 3 μm ($n = 3$ experiments; 200–300 synaptosomes analysed by experiment).

### *3.2. Immunochemical characterization of P2X receptors in rat cerebellar synaptosomal preparations*

The immunological characterization of P2X receptor subunits present at pre-synaptic level with the antibodies available for $P2X_1$, $P2X_2$, $P2X_3$, $P2X_4$, $P2X_5$, $P2X_6$ and $P2X_7$, showed that only the anti-$P2X_3$ and the anti-$P2X_7$ antibodies positively and abundantly labelled rat cerebellar synaptic terminals (Fig. 2A–F). Much discussion exists concerning the specificity of $P2X_7$ antibodies [27]. With regard to this item, when these antibodies were tested against synaptosomal membranes, two main protein bands were detected, with molecular weight in the range of what described for $P2X_7$ ($n = 3$; Fig. 2G). The degree of co-localization of $P2X_3$ and $P2X_7$ subunits, with the synaptic vesicular marker synaptophysin was studied. It was found

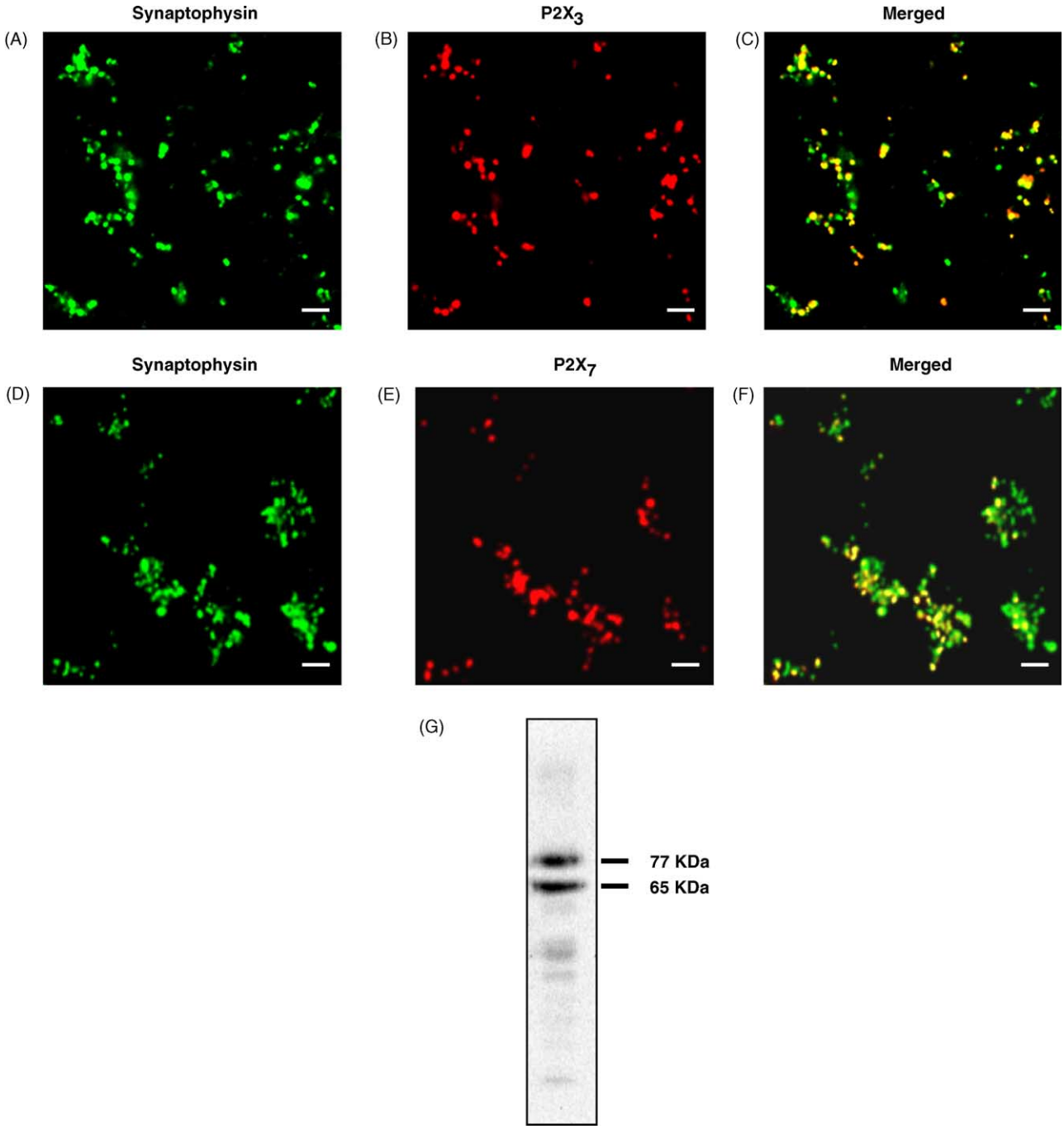


Fig. 2. Presence of $P2X_3$ and $P2X_7$ receptor subunits in rat cerebellar synaptic terminals. (A and D) Fluorescence images of rat cerebellar synaptic terminals labelled with mouse anti-synaptophysin and tagged with goat anti-mouse IgG fluorescein conjugate. The same fields presented in images (A and D) are, respectively, shown with guinea pig anti-$P2X_3$ (B) and rabbit anti-$P2X_7$ (E) tagged with goat anti-guinea pig IgG rhodamine conjugate (B) and goat anti-rabbit IgG rhodamine conjugate (E). Co-localization of each P2X subunit with synaptophysin is shown (C and F). Scale bars = 5 μm ($n = 3$ experiments; 200–300 synaptosomes analysed by experiment). (G) Western blot with $P2X_7$ antibody in rat cerebellar synaptosomes. Cerebellar synaptosomes were subjected to SDS-page 10% electrophoresis and western blotting protocol as is described in Section 2. The $P2X_7$ antibody detected two main size bands, with 77 and 65 kDa ($n = 3$).

$28 \pm 4\%$ of terminals labelled for $P2X_3$ subunit and a higher percentage of terminals, reaching the $60 \pm 5\%$ of the total, labelled for $P2X_7$ subunit ($n = 3$). The high percentage of $P2X_7$ labelling at the pre-synaptic level may also include other proteins exhibiting regional homology, as the one in Fig. 2G.

The presence of $P2X_2$ subunits was restricted to a very scarce percentage of synaptosomes (<2%) ($n = 3$; Fig. 3A and B). The immunochemical experiments carried out with the anti-$P2X_1$, anti-$P2X_4$, anti-$P2X_5$ and anti-$P2X_6$ antibodies showed no positive labelling in cerebellar synaptic terminals ($n = 3$; results not shown), even though the quality of the antibodies has been previously reported [25]. It is to notice that $P2X_1$ labelling was very abundant in cerebellar granule cells maintained during 14 days in culture ($n = 3$; Fig. 3E–G), where it exhibited a continuous

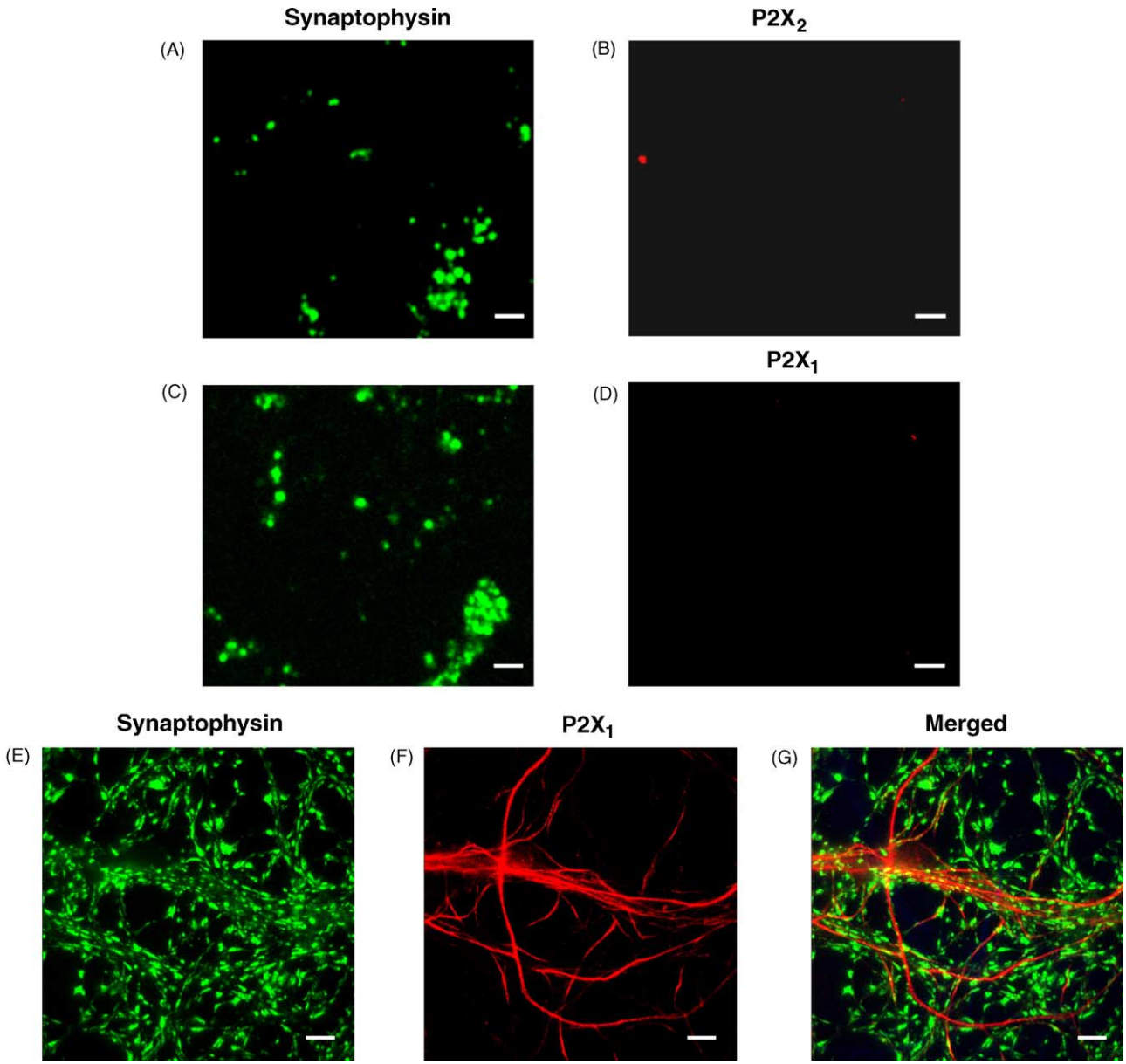


Fig. 3. Immunocytochemistry of $P2X_1$ and $P2X_2$ receptor subunits in rat cerebellar granule cells and synaptic terminals. (A and C) Fluorescence images of rat cerebellar synaptic terminals labelled with mouse anti-synaptophysin and tagged with goat anti-mouse IgG fluorescein conjugate. The same fields presented in images (A and C) are, respectively, shown with guinea pig anti-$P2X_2$ (B) and rabbit anti-$P2X_1$ (D), tagged with goat anti-guinea pig IgG rhodamine conjugate (B) or goat anti-rabbit IgG rhodamine conjugate (D). (E) Fluorescence image of rat cerebellar granule cells (14 DIV) labelled with mouse anti-synaptophysin and tagged with goat anti-mouse IgG fluorescein conjugate. The same field as (E) shown with rabbit anti-$P2X_1$ and tagged with goat anti-rabbit IgG rhodamine conjugate (F). Co-localization of $P2X_1$ subunit with synaptophysin is shown in (G). Scale bars = 5 μm ($n$ = 3 experiments; 200–300 synaptosomes analysed by experiment).

distribution on the neuronal prolongations, although it did not co-distribute with synaptophysin. This fact could explain the absence of immunolabelling for the $P2X_1$ at the cerebellar synaptic terminals ($n$ = 3; Fig. 3C and D).

The immunolabelling of different P2X subunits at the pre-synaptic terminals indicates the presence of the protein but does not give information concerning their functionality. To approach this specific issue microfluorimetric techniques were used.

### 3.3. $Ca^{2+}$ responses evoked by ATP and α,β-methylene-ATP in single cerebellar synaptic terminals

Rat cerebellar synaptosomes were tested for their ability to mobilize $Ca^{2+}$ after stimulation with ATP or α,β-meATP in HBM medium which contains $Mg^{2+}$, as described in Section 2. In all cases, synaptic terminals were superfused with a 30 mM KCl pulse at the end of the experiment in order to confirm synaptosomal functionality. The mean response in $Ca^{2+}$ increase in cerebellar synaptic terminals

once challenged with ATP was 91.6 ± 11.9 nM, exhibiting a pronounced decay after reaching the maximal response. This ATP response was exclusively due to extracelullar calcium entry because there was no response when EGTA was present in the medium ($n = 4$; Fig. 4A). Once demonstrated the response to ATP, the desensitization of the presynaptic P2X receptors was studied by applying a second pulse of the agonist 1 min later. In this situation, more than half of the synaptic terminals responding to the first stimulus of ATP (60%), were not able to respond to the second application ($n = 4$; Fig. 4B). This indicates that $P2X_1$ or $P2X_3$ receptors might be involved in the ATP response. The existence of terminals containing P2X receptors not subjected to desensitization is shown in Fig. 4C.

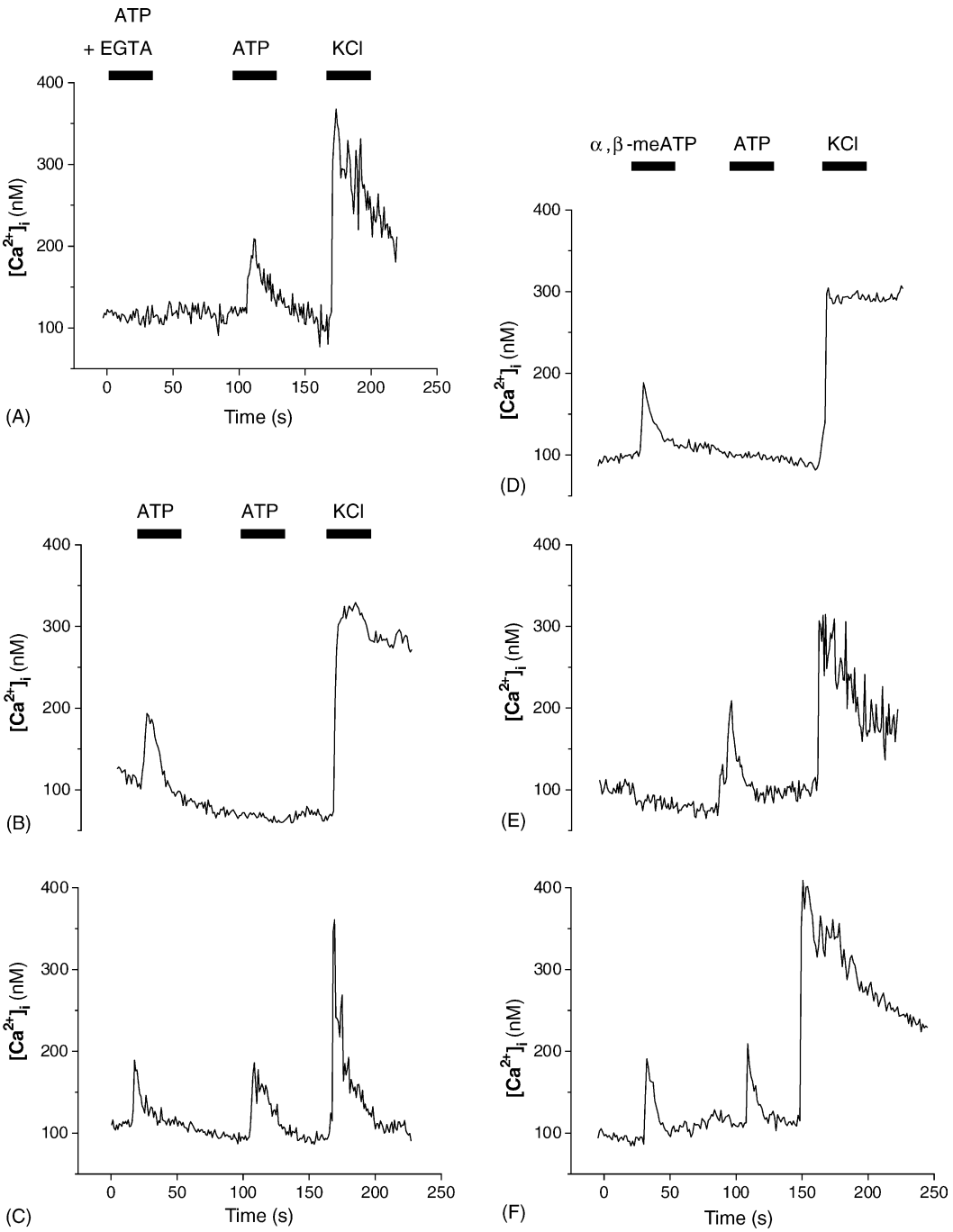


Fig. 4. Responses to ATP and α,β-meATP in single synaptic terminals from rat cerebellum. (A) Rat cerebellar synaptosomes glued to a coverslip mounted in a superfusion chamber were loaded with Fura-2 AM to monitor changes in the intrasynaptosomal $Ca^{2+}$ concentration induced by agonist stimulation: ATP (100 μM), in the presence or absence of EGTA and KCl (30 mM), as described in Section 2. (B) Synaptosomes were stimulated with two pulses of ATP 100 μM, during 30 s each and a time period of 1 min between consecutive stimulations. Two experimental plots, showing responses with desensitization (B) or no-desensitization (C) of the receptors. (D–F) Synaptosomes were challenged with α,β-meATP and ATP, for 30 s each, and a time period of 1 min between consecutive stimulations. The three typical responses obtained are shown. In all cases, bars indicate the time of application of each substance ($n = 4$–5 experiments; 300–400 synaptosomes analysed by experiment).

As the nucleotide analogue, α,β-meATP, is a more specific agonist for the homomeric $P2X_1$ and $P2X_3$, or the heteromeric $P2X_2/P2X_3$ receptors, similar experiments as those with ATP were carried out. The responses recorded in single synaptic terminals after stimulation with α-β-meATP are shown in Fig. 4D–F. The maximal calcium increase was similar to the one induced by ATP and a similar pronounced decay was observed after reaching the maximal response. Heterologous desensitization studies were carried out by applying a second pulse of the agonist ATP 1 min after the previous application, as it is shown in Fig. 4D–F ($n = 4$). More than half of the terminals, responding to α,β-meATP, were not able to respond to a second challenge of nucleotide agonist. In addition it is to emphasize that there are terminals that did not respond to the first stimulation of α,β-meATP, and as a consequence, they were not desensitized to a further ATP response. Thus, pre-synaptic terminals exhibit various possibilities concerning the presence of P2X receptors. As there is no labelling of $P2X_1$ at the pre-synaptic level, $P2X_3$ is one of the most probable receptor to be present in these structures, and capable of desensitization.

To confirm the abundant presence of $P2X_3$ receptors the inhibitory effect of $Ip_5I$ was studied in single synaptic terminals. As shown in Fig. 5A, 50 μM $Ip_5I$ completely blocked the response to α,β-meATP in isolated synaptic terminals ($n = 3$). The same situation occurred when 100 nM $Ip_5I$ was employed (Fig. 5B; $n = 3$). However, when 10 nM $Ip_5I$ was used, a concentration that inhibits $P2X_1$ but not interferes with $P2X_3$, most of the terminals were able to respond to α,β-meATP in the presence of the antagonist (Fig. 5C; $n = 3$). They were also able to respond to a second pulse of α,β-meATP 10 min later, once desensitization period had finished.

### 3.4. Effect of $Mg^{2+}$ ions on the $Ca^{2+}$ responses evoked by ATP in single cerebellar synaptic terminals

Experiments addressed to find functional $P2X_7$ receptors at the pre-synaptic level were performed. In this way and as shown in Fig. 6A, the synaptic terminals were identified according to their responses to ATP in the presence or absence of $Mg^{2+}$. It is generally accepted that deprivation of this ion allows a better response of $P2X_7$ receptors. There were terminals that only respond to ATP in a medium with $Mg^{2+}$, as it was the case of the terminal labelled as 1 ($n = 4$; Fig. 6A and B), as could be expected from the results reported in the former section. There were also synaptic terminals that responded to ATP in $Mg^{2+}$-free medium but not in the presence of this ion, as it was the case of the one labelled as 2 (Fig. 6A and B), these being the most abundant. Besides, other synaptic terminals responded to both pulses of ATP whether in presence or absence of magnesium ions in the medium and the terminal labelled as 3 is an example. Finally, there were terminals that do not show ATP response neither in the presence or

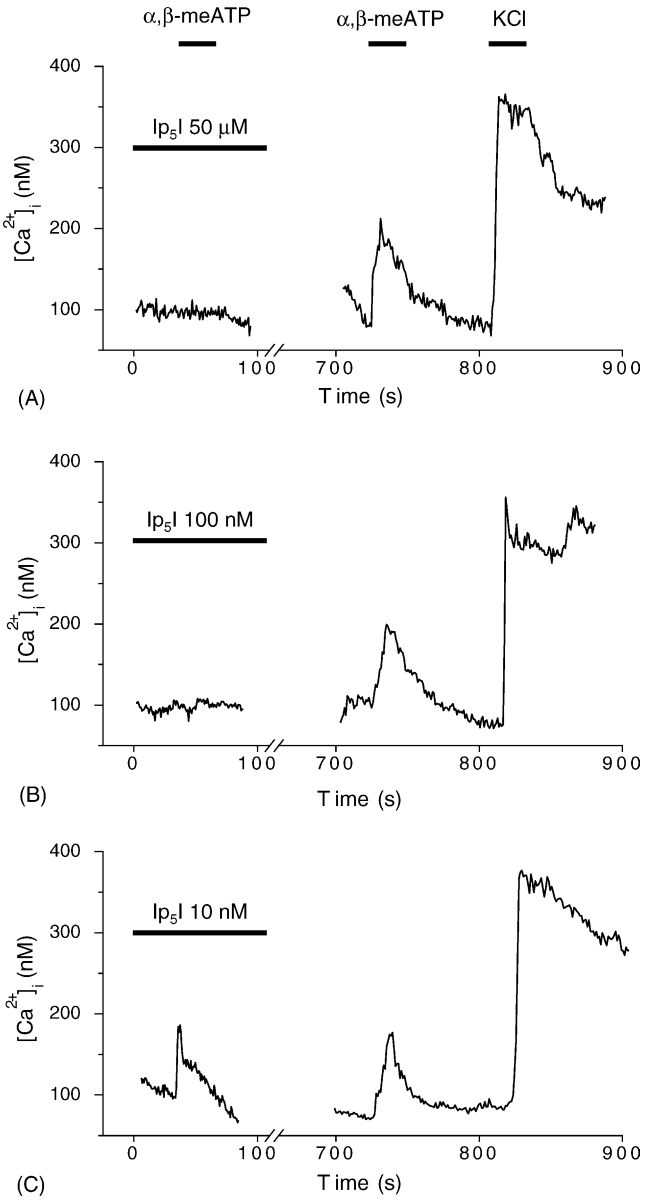


Fig. 5. Effect of $Ip_5I$ on the α,β-meATP responses. Intrasynaptosomal calcium increase induced by 100 μM α,β-meATP was measured in the presence of $Ip_5I$. Several antagonist concentrations were tested (50 μM, 100 and 10 nM). (A) Time course plot of the intrasynaptosomal calcium concentration recorded from a representative single synaptic terminal. The antagonist $Ip_5I$ 50 μM was applied 2 min before and during the agonist stimulation. Synaptosomes were washed for at least 10 min before applying a second pulse with the agonist α,β-meATP. This time is enough to let receptors to recover from their desensitization period. At the end, a pulse of 30 mM KCl was applied to test synaptosomal functionality. Stimulation period is indicated by solid bars. (B and C) An experiment similar to that showed in (A) but with an antagonist concentration of 100 and 10 nM, respectively. The number of individual synaptic terminals under study was 300–400 per experiment ($n = 3$).

absence of $Mg^{2+}$ ions. This lack of response could be due to several factors: first, the absence of nucleotide receptors, second, a response below the limit of detection, or third, the presence of receptors being activated by different nucleotide agonists, or exhibiting very specific requirements. These results confirm the ones reported in previous section

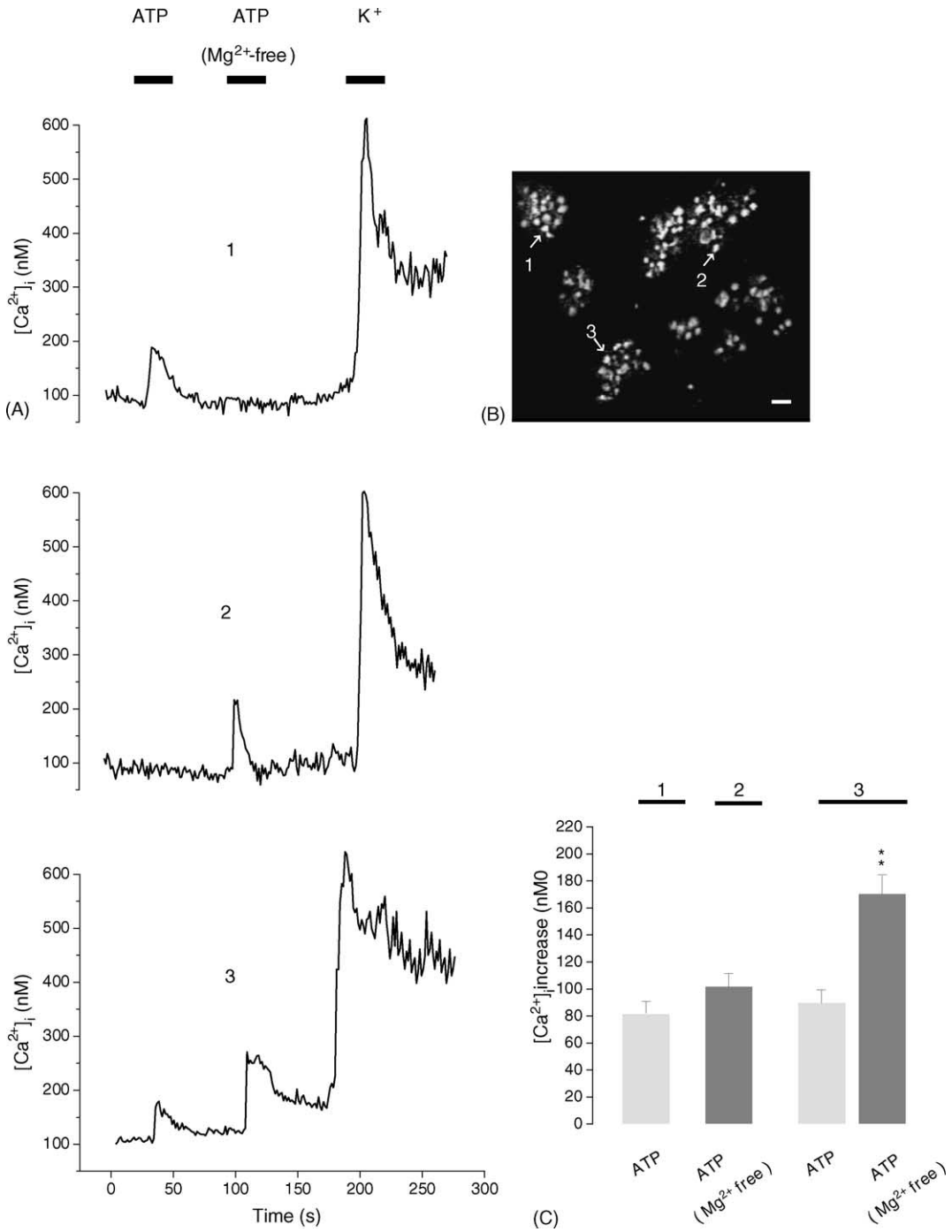


Fig. 6. Responses to ATP in the absence or presence of $Mg^{2+}$ ions in single synaptic terminals from rat cerebellum. Rat cerebellar synaptosomes glued to a coverslip mounted in a superfusion chamber were loaded with Fura-2 AM to monitor changes in the intrasynaptosomal $Ca^{2+}$ concentration induced by ATP (100 μM), in the presence or absence of $Mg^{2+}$, and KCl (30 mM), as described in Section 2. (A) Representative traces show the time course of intrasynaptosomal calcium concentration recorded from the terminals labelled as 1–3 in the fluorescence image of synaptosomes loaded with Fura-2 (and shown in B). Bars indicate the time of application of each substance. Scale bar = 3 μm. (C) Calcium concentration increases induced by ATP in the presence or absence of $Mg^{2+}$ in synaptic terminals, that correspond, respectively, to the response types 1–3 shown in panel (A). Each bar represents the mean ± S.E.M. of four experiments performed in different synaptosomal preparations, and 300–400 synaptosomes were analysed by preparation. $^{**}p < 0.01$, very significantly different from the mean of the response to ATP in population 3, using one tailed Student′s paired test.

concerning the complexity of nucleotide responses at the pre-synaptic level.

Considering the single synaptic terminals responses from the experimental situation reported in Fig. 6A, the terminals responding exclusively to ATP in the absence of $Mg^{2+}$ (type 2), accounted for three times higher number with respect the other types. It is to notice that the high number of terminals responding to ATP in $Mg^{2+}$-free medium supports the abundant existence of functional $P2X_7$.

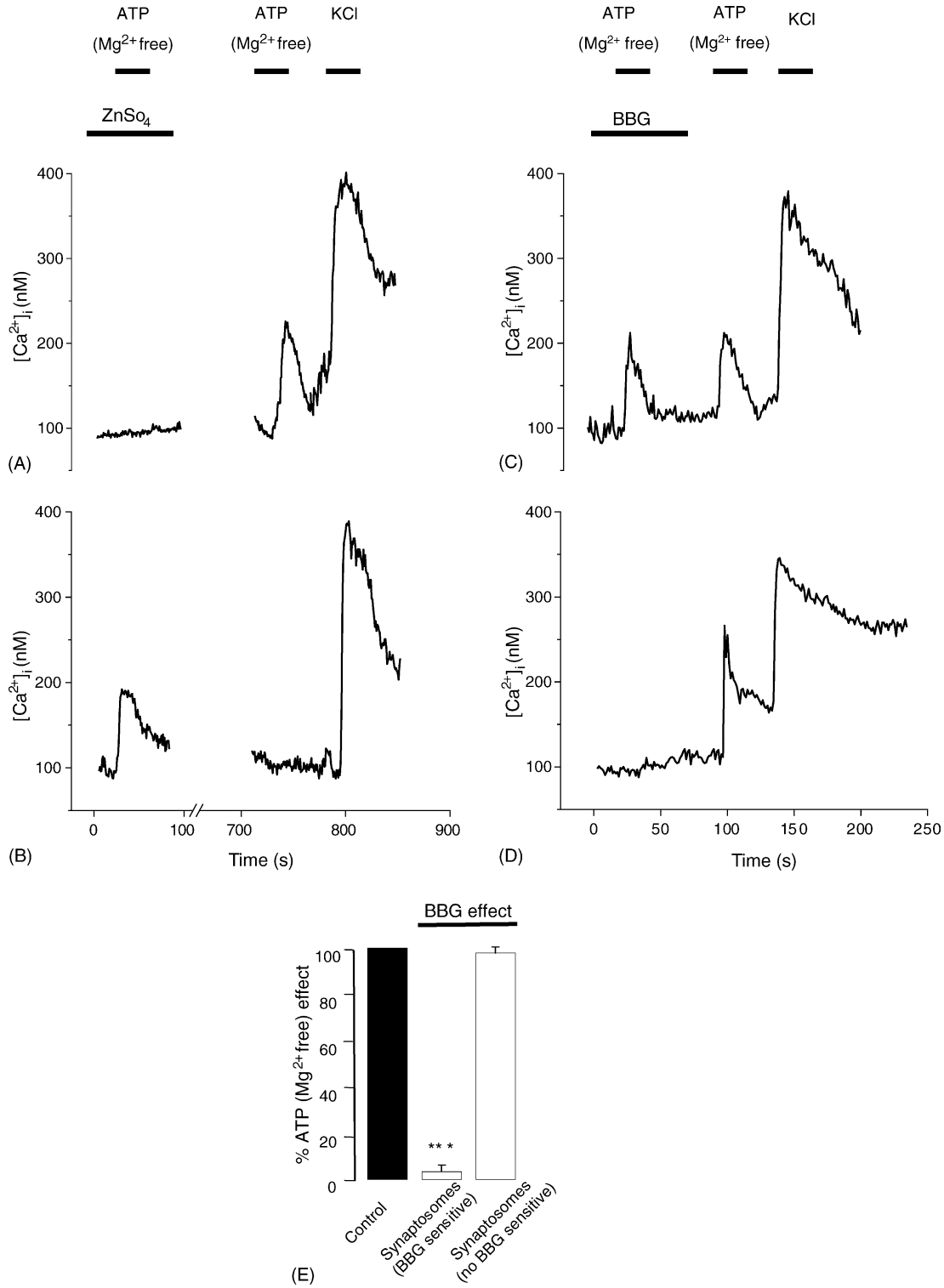


Fig. 7. Effect of $Zn^{2+}$ and Brilliant Blue G on the ATP responses in the absence of $Mg^{2+}$. Intrasynaptosomal calcium increase induced by 100 μM ATP in the absence of $Mg^{2+}$ ions was measured in the presence of 100 μM $ZnSO_4$ or 1 μM Brilliant Blue G. (A and B) Time course plot of the intrasynaptosomal calcium concentration recorded from two representative single synaptic terminals. $ZnSO_4$ was applied 2 min before and during the agonist stimulation. Synaptosomes were washed for 10 min before a second pulse with the agonist (ATP 100 μM in a free-$Mg^{2+}$ medium). (C and D) Two plots showing the effect of BBG on the ATP response in the absence of $Mg^{2+}$. BBG was applied 2 min before and during the agonist stimulation. Synaptosomes were washed for 1 min to retire the antagonist before stimulating again with the agonist (ATP 100 μM in a free-$Mg^{2+}$ medium). At the end of all experiments, a pulse of 30 mM KCl was applied to test synaptosomal functionality. Stimulation period is indicated by solid bars. (E) Values of $[Ca^{2+}]_i$ increase are represented as a percentage of intrasynaptosomal calcium increase induced by 100 μM ATP when applied alone (100%) or in the presence of BBG. Assays were performed in a medium free of $Mg^{2+}$ ions. Data are mean ± S.E.M. of three experiments in different synaptosomal populations. $^{***}p < 0.001$, differences extremely significant from the mean of the response to ATP in the control, using one tailed Student's paired test. The number of individual synaptic terminals under study is 300–400 per experiment.

It is noteworthy to say that the $Ca^{2+}$ response intensity elicited by ATP (with or without $Mg^{2+}$ in the medium) varied between terminals. Calibration of fluorescence ratio to get intrasynaptosomal concentration $[Ca^{2+}]_i$ (see Section 2), showed a basal value of $85.6 \pm 7.2$ nM. The $Ca^{2+}$ increase induced by ATP and ATP without $Mg^{2+}$, at 100 μM concentration, in terminals responding only to one of these agonists, showed values of $87.4 \pm 10.9$ and $109.4 \pm 12.7$ nM, respectively. However, terminals that responded to ATP, both in the presence and absence of $Mg^{2+}$, exhibit an ATP response in the absence of this ion significantly higher than the one for ATP with $Mg^{2+}$, being $183.2 \pm 17.7$ and $96.3 \pm 12.1$ nM, respectively (Fig. 6C). These values were not modified when ATP-free $Mg^{2+}$ was the first agonist to be used in the perfusion system (results not shown).

As $Zn^{2+}$ ions have been described as inhibitors of $P2X_7$ receptors, studies were carried out in the presence of $ZnSO_4$. In Fig. 7A, it can be observed that $Zn^{2+}$ ions completely abolished the ATP response in the absence of $Mg^{2+}$. These data correspond to a classical $P2X_7$ receptor. However, the terminals responding to $Mg^{2+}$-free ATP, when $Zn^{2+}$ ions were present, did not respond in the absence of this ion (Fig. 7B). This behaviour has been reported for $P2X_3$ receptors, where $Zn^{2+}$ ions improve the response.

The effect of Brilliant Blue G (BBG), a selective antagonist for $P2X_7$ receptors, was measured in single terminals. The antagonist was applied in HBM medium, and it was kept in contact with synaptic terminals in the perfusion chamber for a period of 2 min before, and during the first pulse with the agonist. ATP without $Mg^{2+}$ was always employed as the agonist in these experiments. To check the recovery after inhibitory treatment the terminals were washed for another minute with HBM media and challenged again with a second pulse of ATP in the absence of $Mg^{2+}$. The inhibition range can only be quantified when the inhibitory effects are studied in single synaptic terminals, with experiments as those reported in Fig. 7C and D, which shows typical experimental recordings. This technique has allowed us to identify two different populations according to the BBG effect. In one population, the response to 100 μM ATP in the absence of $Mg^{2+}$ was completely inhibited by BBG 1 μM, accounting for the $47 \pm 11\%$ of synaptosomes ($n = 3$; Fig. 7E). In the other population, BBG did not have inhibitory effect and corresponds to $50 \pm 8\%$ of synaptosomes ($n = 3$; Fig. 7E). These results as the ones in the previous section points to the large variety and possibilities of nucleotide receptors at the pre-synaptic level.

### 3.5. Dose–response curves for ATP and BzATP in single terminals

Microfluorimetric techniques have also allowed to carry out the dose–response curves in single terminals. Synaptic terminals were challenged with increasing concentrations of the agonists ATP and BzATP between 1 nM and 1 mM in the perfusion medium. The experiments were carried out in the presence or absence of magnesium ions, and the curves obtained have been represented in Fig. 8 ($n = 3$–4). The dose–response curves showed some differences in affinity and maximum effect with $Mg^{2+}$ withdrawal. Concerning ATP, $EC_{50}$ values were $39.4 \pm 0.4$ μM in the presence of $Mg^{2+}$ and close to two orders of magnitude lower, $0.3 \pm 0.1$ μM, in a free-$Mg^{2+}$ medium. Besides, the maximum effect for ATP without $Mg^{2+}$ was higher than that obtained in the presence of the ion, with calcium values of $132.8 \pm 12.9$ and $91.6 \pm 11.9$ nM, respectively

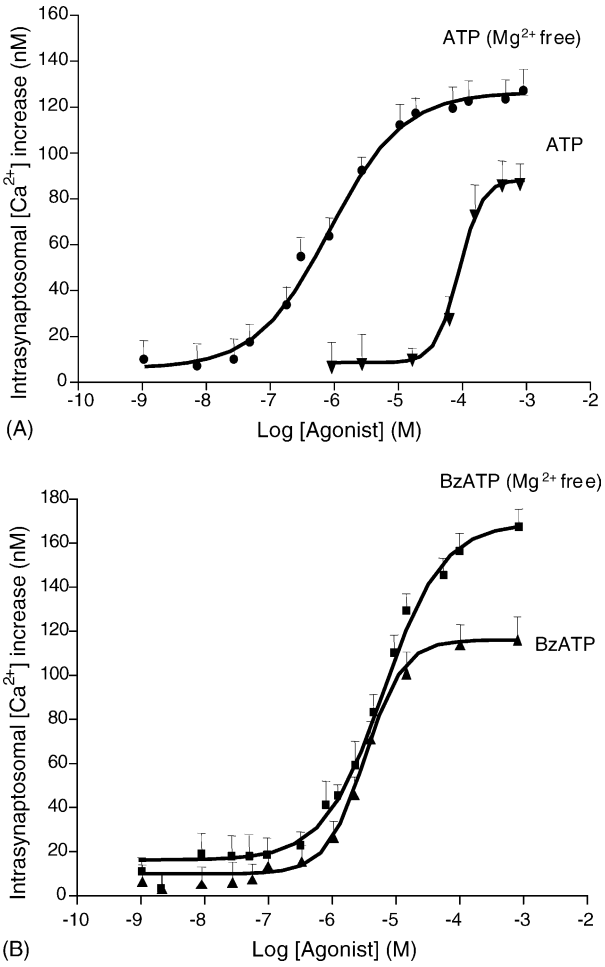


Fig. 8. Dose–response curves for ATP and BzATP in single synaptic terminals from rat cerebellum. Dose–responses curves for ATP or BzATP were obtained both in the presence of 1 mM $Mg^{2+}$or in the absence of such ion. Synaptosomes isolated from rat cerebellum and glued to a coverslip mounted in a superfusion chamber were loaded with Fura-2 AM. Changes in the intrasynaptosomal $Ca^{2+}$ concentration induced by graded doses of ATP in the presence or absence of $Mg^{2+}$(A), or BzATP in the presence or absence of $Mg^{2+}$(B), concentrations ranging from 1 nM to 1 mM, were monitored. Synaptic terminals were stimulated with 30 mM KCl at the end of the experiment to test their functionality. Calcium increase values are the mean ± S.E.M. for each agonist concentration of at least three experiments performed in different synaptosomal preparations ($n = 3$–4) and number of individual synaptic terminals tested between 315 and 457.

Table 1
$EC_{50}$ values, maximal response and Hill numbers for ATP and BzATP concentration–response curves in the absence or presence of $Mg^{2+}$ in synaptic terminals from rat cerebellum

| | | $EC_{50}$ (μM) | Maximal response (nM) | $n_H$ |
|---|---|---|---|---|
| ATP (+$Mg^{2+}$) | $n = 3$ ($n' = 315$) | 39.4 ± 0.4 | 91.6 ± 11.9 | 1.66 ± 0.26 |
| ATP ($Mg^{2+}$ free) | $n = 4$ ($n' = 443$) | 0.3 ± 0.1 | 132.9 ± 12.9 | 0.63 ± 0.10 |
| BzATP (+$Mg^{2+}$) | $n = 3$ ($n' = 364$) | 1.4 ± 0.5 | 104.3 ± 9.4 | 1.20 ± 0.47 |
| BzATP ($Mg^{2+}$ free) | $n = 4$ ($n' = 457$) | 4.2 ± 0.9 | 169.7 ± 17.1 | 0.77 ± 0.11 |

Data are expressed as the $EC_{50}$ values (concentration of agonist producing 50% of the maximal response) and maximal responses induced by ATP and BzATP in the different experimental conditions. $n_H$ is the Hill coefficient. Data represents the mean ± S.E.M. ($n$ = number of experiments; $n'$ = total of synaptosomes tested).

(Fig. 8A). In a similar way as happened with ATP, the maximum effect induced by BzATP was higher in free-$Mg^{2+}$ conditions, the values being 104.3 ± 9.3 and 169.6 ± 17.1 nM in the presence or absence of the ion, respectively (Fig. 8B).

Concerning the Hill number both nucleotides in the presence of $Mg^{2+}$ exhibit a slight co-operative behaviour no observable in the absence of the ion. The values of $EC_{50}$, maximum effect and Hill number are summarized in Table 1.

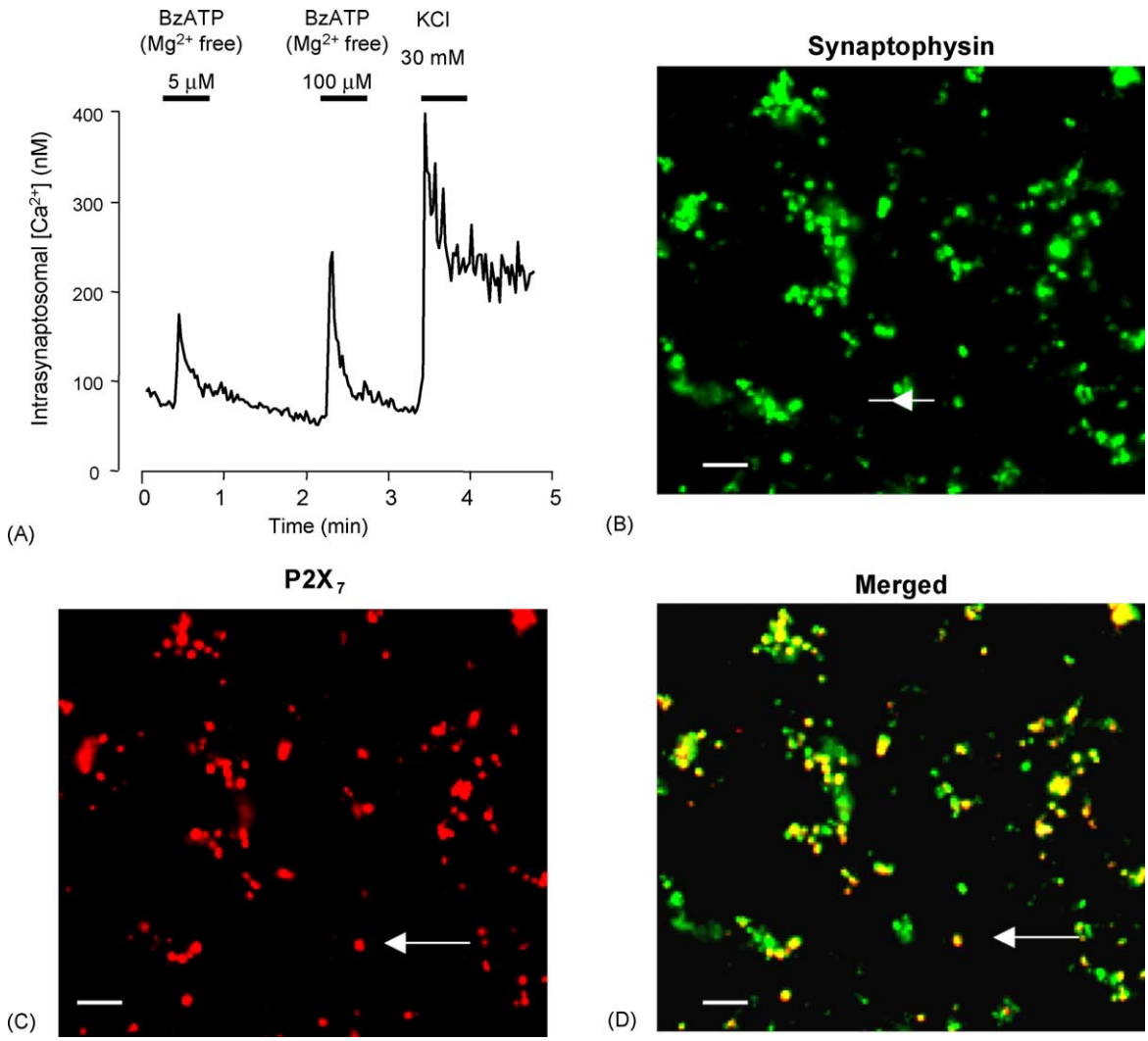


Fig. 9. Correlation between BzATP responses in the absence of $Mg^{2+}$ ions and presence of $P2X_7$ subunits in single synaptic terminals. Rat cerebellar synaptosomes glued to a coverslip mounted in a superfusion chamber were loaded with Fura-2 AM to monitor changes in the intrasynaptosomal $Ca^{2+}$ concentration induced by stimulation with two different concentrations of BzATP (5 and 100 μM), in the absence of $Mg^{2+}$ ions. A pulse of KCl (30 mM) was applied at the end of the experiment to confirm synaptosomes functionality. After these studies synaptosomes were fixed with *p*-formaldehyde for immunocytochemical characterization. (A) Time course of Fura-2 fluorescence emission changes recorded for the terminal indicate with an arrow in panel B. Solid bars indicate the period while each substance was applied. (B) Fluorescence image of synaptophysin-FITC labelled synaptosomes. (C) Same field as (B) labelled with anti-$P2X_7$ antibodies and tagged with anti-rabbit-TRICT-coupled secondary antibodies. (D) Co-localization of $P2X_7$ subunit with synaptophysin is shown ($n = 3$; bar = 5 μm).

### 3.6. Correlation between BzATP responses in the absence of $Mg^{2+}$ and immunolabelling of $P2X_7$ receptors in single terminals

To determine whether a co-localization between $P2X_7$ immunolabelling and the calcium responses to the better $P2X_7$ agonist (BzATP in the absence of $Mg^{2+}$) occurs, we combined microfluorimetric studies with immunocytochemical assays.

Isolated synaptic terminals loaded with Fura-2 AM were stuck on microgrid coverslips (square size 55 μm) to relocate individual synaptosomes after immunostaining procedures. Synaptosomes were tested for their ability to mobilize $Ca^{2+}$ in response to BzATP in the absence of $Mg^{2+}$. Two consecutive pulses with the nucleotide, the first of 5 μM and the second one of 100 μM, were employed, with 30 s duration and no less than 1 min time interval between applications (Fig. 9A). The 5 and 100 μM BzATP concentrations were selected because they correspond to values close to one and twenty times the $EC_{50}$ value, respectively. After functional studies synaptosomes were fixed and labelled with antibodies that recognize specifically either the vesicular protein synaptophysin or the $P2X_7$ receptor ($n = 3$; Fig. 9B–D).

These analyses showed that the great majority of the synaptic terminals responding to BzATP in the absence of $Mg^{2+}$, 91 ± 6%, were further positively labelled with the anti-$P2X_7$-subunit antibody.

## 4. Discussion

The present study demonstrates the existence and large variety of functional P2X receptors in rat cerebellar synaptosomal preparations by means of immunocytochemical and microfluorimetric techniques.

In cerebellum, 90% of neurons are granule cells, which contact Purkinje neurons using glutamate as excitatory neurotransmitter. According with this feature, a high percentage that accounts for two thirds of the total number of synaptic terminals, isolated from rat cerebellum, have glutamatergic phenotype. This approach is taking into consideration that in most CNS regions, VGLUT1 and VGLUT2 expression appears not to overlap, defining separate populations of synaptic terminals in adult animals [32,33]. This distribution is consistent with our previous studies that showed abundant and punctate VGLUTl and VGLUT2 labelling in cerebellar granule cells [25]. In cerebellum, there are also terminals that exhibit GABAergic phenotype, labelled with anti-GAD antibodies, accounting for about one-third of the total. This result agrees with the existence of Purkinje, stellate, basquet and Golgi neurons in cerebellum, which are GABAergic. VGLUT1 and GAD labelling does not overlap, showing that the glutamatergic or GABAergic phenotype does not co-exist in the same terminal.

Results from immunocytochemical and microfluorimetric techniques, demonstrated the presence and functionality of various P2X receptors in cerebellar preparations. Some comments are necessary concerning the $P2X_1$ subunit, which was not detected by immunolabelling at the pre-synaptic level. However, in the same experimental conditions reported here, $P2X_1$ immunolabelling clearly appears in whole granule cells in culture with the same antibody, but not exhibiting co-distribution with the synaptic marker synaptophysin. Presence of $P2X_1$ immunolabelling has also been described in the varicosities of cerebellar parallel fibers and other CNS regions [3,8,34]. Functional homomeric $P2X_1$ receptors have been reported in rodent vas deferens and smooth muscle tissue [5]. These data are relevant concerning the pre-synaptic calcium responses to α,β-meATP, and the P2X subunits mediating the response.

By immunolabelling, $P2X_3$ receptor subunits are detected in a percentage close to one quarter of the total cerebellar synaptic terminals. The presence of $P2X_3$ subunits has been reported in many areas of central nervous system, such as at the hypothalamic supraoptic nucleus and solitary tract nucleus, and at the pre-synaptic level of nerve terminals of sensory pathways to the spinal cord dorsal horn, and also at the peripheral endings [3,8,35]. Synaptic terminals from rat midbrain also exhibit abundant labelling by $P2X_3$ antibodies [31]. It is relevant to emphasize that in cultured granule cells $P2X_3$ labelling co-distributes with the vesicular pre-synaptic marker synaptophysin [25]. In this model, the presence of $P2X_2$ subunit appears more restricted to the cell soma, as it is also the case for $P2X_4$. Only scarce terminals are immunolabelled for $P2X_2$ subunit in our model, being $P2X_4$ subunit not detectable at the pre-synaptic level. Similar abundance and distribution of $P2X_2$ and $P2X_3$ subunits have been reported in sensory nerve endings, which is not the case in cerebellar synaptic terminals [36,37].

The characterization with anti-$P2X_7$ antibodies is submitted to much controversy, since it has been reported that the $P2X_7$-KO mice exhibits the same labelling characteristics in brain tissues for this subunit, as the wild animal [26]. It is possible that, in cerebellar synaptic terminals, in addition to the whole length $P2X_7$ labelling protein, other analogous proteins containing the antigenic epitope could be responsible for the additional band detected by western studies. This could explain the abundant presence of more than half of the total terminals that exhibit $P2X_7$ labelling.

Microfluorimetric studies of calcium responses in single synaptic terminals are necessary to confirm the existence of functional P2X receptors at the pre-synaptic level. On the basis of the P2X subunits present at the synaptic terminals, the responses to α,β-meATP and the desensitization results agree with the existence of functional homomeric $P2X_3$ receptors. As, in the presence of $Mg^{2+}$ ions, more than half of the ATP and α,β-meATP responding terminals, exhibit homologous or heterologous desensitization, the abundant

presence of $P2X_3$ subunits assembled as homomeric receptors can be inferred at the pre-synaptic level. Moreover, the existence of no-desensitising nucleotide responses also indicates the presence of heteromeric $P2X_2/P2X_3$ or homomeric $P2X_2$ receptors located at the pre-synaptic level [5,8,35,36,38,39]. However, it is to take into account the scarce presence of $P2X_2$ subunits detected by immunocytochemistry. Presence of functional $P2X_3$ homomeric and $P2X_2/P2X_3$ heteromeric receptors has also been reported in midbrain synaptic terminals [31,40]. At this respect, the inhibitory effect of $Ip_5I$, and the concentration required for such inhibition confirms the presence of $P2X_3$ receptors at the pre-synaptic level in rat cerebellum [30]. The presence of other P2X receptors not yet cloned, or the currently described but post-transcripcionally modified, needing more specific functional requirements, are not excluded at the pre-synaptic level.

In cerebellar synaptic terminals, the abundant presence of $Ca^{2+}$ responses to ATP or BzATP that improve when $Mg^{2+}$ ions are not present, agrees with the $P2X_7$ phenotype, and as reported here, more than half of these structures exhibit $P2X_7$ or $P2X_7$-like immunolabelling. The inhibitory $Mg^{2+}$ effect can be explained by an allosteric inhibition mediated by divalent ions binding the receptor, among other hypothesis [41]. However, it is to emphasize that dose–response curves showed cooperativity when $Mg^{2+}$ was present. This effect could be understood as a way to optimize the effect of the ATP with respect to $ATP^{4-}$, a less abundant molecular form in natural conditions.

The fact that BzATP is more potent than ATP in our cerebellar preparations is another distinctive feature of $P2X_7$ receptors, according with the effect of BzATP described by other authors [16]. Although BzATP is an effective agonist at other P2X receptors, in particular, $P2X_1$, $P2X_2$ and $P2X_3$, it is only at the $P2X_7$ receptor that BzATP is more potent than ATP [5].

The inhibitory effect of $Zn^{2+}$ ions in the absence of $Mg^{2+}$ agrees with the presence of $P2X_7$ receptors at the synaptic terminals [41]. Moreover, in terminals where no responses to ATP were observed, $Zn^{2+}$ was able to induce a response to this agonist, indicating that a more favourable situation for a $P2X_3$ response was being established, thus confirming once more the presence of $P2X_3$ receptors at the pre-synaptic level [42].

Studies with Brilliant Blue G, a selective $P2X_7$ antagonist [43], well agrees with other works about the $P2X_7$ antagonism, inhibiting calcium influx induced by ATP in the absence of $Mg^{2+}$ at concentrations previously reported to be effective [44,45]. The concentration used is expected to produce low inhibitory effect on rat $P2X_2$ receptors; in addition, this subunit is scarcely expressed in the cerebellar synaptosomes. Moreover, it is to take into account that half of the responses were completely abolished by BBG, as it could be expected from the $P2X_7$ properties reported in the literature [13,22,23,41]. However, no inhibition at all was observed on the other half of the ATP-$Mg^{2+}$ free responding terminals. These data agree, once more, with the great heterogeneity of P2X receptors present at the nucleotide responding terminals.

In addition to the functional properties present in $P2X_7$ receptors in cerebellum, their particular subcelullar distribution also resembles that found in other systems. $P2X_7$, or its brain analogue, is usually expressed in a dotting pattern, indicating association with specialized structures at synapsis [12,14–16,46]. In contrast with other P2X subunits that can be found pre-synaptically and postsynaptically, $P2X_7$ receptors are more prevalent at pre-synaptic sites [13,23]. Since the pre-synaptic nerve terminal is a fundamental regulatory site to control and modulate neurosecretion, the pre-synaptic $P2X_7$, or $P2X_7$-like, characteristic distribution suggests a prominent role of $P2X_7$ in the signalling of cerebellum.

In addition, $P2X_7$ receptors are mainly targeted to excitatory terminals of neurons, associated with VGLUT1 and/or VGLUT2 glutamatergic markers. In fact, $P2X_7$ subunits co-localize with both VGLUT1 and VGLUT2 at the granular layer in cerebellum. However, in certain brainsteam and spinal cord nuclei the $P2X_7$ may be adittionally expressed by subpopulations of cholinergic and GABAergic/glycinergic terminals, suggesting a role in neurotransmission in different synaptic terminals [22].

However, it is not clear how the high ATP concentrations necessary to activate the $P2X_7$ receptor could reach the synaptic cleft. On one hand, ATP released from damaged cells or under inflammatory conditions could be a possible source to achieve high local ATP concentrations, in millimolar range, required to activate $P2X_7$ receptors taking into account that $Mg^{2+}$ ions are present in extracellular media surrounding neurons. ATP is also released from neural tissues under ischemia or anoxia [47]. $P2X_7$ may also play an important role in excitotoxicity in response to cellular damage by increasing glutamate release and it could be a therapeutic target to reduce stress induced cell death and in neurodegenerative diseases [48,49].

As ATP is released with other neurotransmitters at the synapsis, this could be the way to achieve the high concentration of ATP necessary to activate the receptor in a restricted and small region near the $P2X_7$ receptor. The fact that $P2X_7$ is expressed close to glutamate transporters and the evidences that ATP evokes glutamate release in cerebellar granule cells [50] supports the hypothesis that $P2X_7$ would be guaranteeing or reinforcing the neurotransmission. The calcium increases mediated by $P2X_7$ could further induce more glutamate release or initiate second messenger cascades that might lead to synapsis reorganization. But in an opposite way, activation of $P2X_7$ present at mossy fibers in the rat hippocampus produced a long-lasting inhibition of neurotransmission, maybe as a protection mechanism when neurotransmission is unusually high [14], suggesting that $P2X_7$ receptor accomplishes for diverse roles in different synapsis.

The pre-synaptic distribution of P2X receptors, mainly those of $P2X_3$ and $P2X_7$ containing subunits, could indicate a role in synergist action with other neurotransmitter receptors regulating synaptic transmission efficiency. Interactions with metabotropic, such as $GABA_B$ and adenosine A1 and A2 receptors as also with ionotropic, such as nicotinic and $GABA_A$ receptors, have been described for the P2X receptors at the pre-synaptic level [37,51–53]. The cross-talk among P2X and other metabotropic and ionotropic receptors may be contributing to long-term plasticity in response to neuronal activity, at the pre-synaptic level.

## Acknowledgements

This work was supported by research grants from the Spanish Ministry of Science and Technology BFI2002-03626) and the C.A.M. (SAL/0551/2004). We would like to thank Dr. J. Gualix for the synthesis and supply of $Ip_5I$.

## References

[1] Ralevic V, Burnstock G. Receptors for purines and pyrimidines. Pharmacol Rev 1998;50:413–92.
[2] North RA, Surprenant A. Pharmacology of cloned P2X receptors. Annu Rev Pharmacol Toxicol 2000;40:563–80.
[3] Nörenberg W, Illes P. Neuronal P2X receptors: localisation and functional properties. Naunyn-Schmiedebergs Arch Pharmacol 2000;362:324–39.
[4] Torres GE, Egan TM, Voigt MM. Hetero-oligomeric assembly of P2X receptor subunits. Specificities exist with regard to possible partners. J Biol Chem 1999;274:6653–9.
[5] North RA. Molecular physiology of P2X receptors. Physiol Rev 2002;82:1013–67.
[6] Edwards FA, Gibb AJ, Colquhoun D. ATP receptor-mediated synaptic currents in the central nervous system. Nature 1992;359:144–7.
[7] Pankratov Y, Castro E, Miras-Portugal MT, Krishtal O. A purinergic component of the excitatory postsynaptic current mediated by P2X receptors in the CA1 neurons of the rat hippocampus. Eur J Neurosci 1998;10:3898–902.
[8] Illes P, Ribeiro JA. Molecular physiology of P2 receptors in the central nervous system. Eur J Pharmacol 2004;483:5–17.
[9] Pintor J, Miras-Portugal MT. A novel receptor for diadenosine polyphosphates coupled to calcium increase in rat midbrain synaptosomes. Br J Pharmacol 1995;115:895–902.
[10] Gómez-Villafuertes R, Gualix J, Miras-Portugal MT, Pintor J. Adenosine 5′-tetraphophate ($Ap_4$), a new agonist on rat midbrain synaptic terminal P2 receptors. Neuropharmacology 2000;39:2381–90.
[11] Díaz-Hernández M, Pintor J, Castro E, Miras-Portugal MT. Independent receptors for diadenosine pentaphosphate and ATP in rat midbrain single synaptic terminals. Eur J Neurosci 2001;14:918–26.
[12] Miras-Portugal MT, Díaz-Hernández M, Giráldez L, Hervás C, Gómez-Villafuertes R, Sen RP, et al. $P2X_7$ receptors in rat brain: presence in synaptic terminals and granule cells. Neurochem Res 2003;28:1597–605.
[13] Deuchars SA, Atkinson L, Brooke RE, Musa H, Milligan CJ, Batten TFC. et al. Neuronal $P2X_7$ receptors are targeted to presynaptic terminals in the central and peripheral nervous system. J Neurosci 2001;21:7143–52.
[14] Amstrong JN, Brust TB, Lewis RG, MacVicar BA. Activation of presynaptic $P2X_7$-like receptors depresses mossy fiber-CA3 synaptic transmission through p38 mitogen-activated protein kinase. J Neurosci 2002;22:5938–45.
[15] Sperlágh B, Kofalvi A, Deuchars J, Atkinson L, Milligan CJ, Buckley NJ, et al. Involvement of $P2X_7$ receptors in the regulation of neurotransmitter release in the rat hippocampus. J Neurochem 2002;81:1196–211.
[16] Lundy PM, Hamilton MG, Mi L, Gong G, Vair C, Sawyer TW, et al. Stimulation of $Ca^{2+}$ influx through ATP receptors on rat brain synaptosomes: identification of functional $P2X_7$ receptors subtypes. Br J Pharmacol 2002;135:1616–26.
[17] Gu JG, Macdermott AB. Activation of ATP P2X receptors elicits glutamate release from sensory neuron synapsis. Nature 1997;389:749–53.
[18] Hugel S, Schlichter R. Presynaptic P2X receptors facilitate inhibitory GABAergic transmission between cultured rat spinal cord dorsal horn neurons. J Neurosci 2000;20:2121–30.
[19] Gómez-Villafuertes R, Gualix J, Miras-Portugal MT. Single GABAergic synaptic terminals from rat midbrain exhibit functional P2X and dinucleotide receptors, able to induce GABA secretion. J Neurochem 2001;77:84–93.
[20] Díaz-Hernández M, Pintor J, Castro E, Miras-Portugal MT. Co-localisation of functional nicotinic and ionotropic nucleotide receptors in isolated cholinergic synaptic terminals. Neuropharmacology 2002;42:20–33.
[21] Gualix J, Gómez-Villafuertes R, Díaz-Hernández M, Miras-Portugal MT. Presence of functional ATP and dinucleotide receptors in glutamatergic synaptic terminals from rat midbrain. J Neurochem 2003;87:160–71.
[22] Moores TS, Hasdemir B, Vega-Riveroll L, Deuchars J, Parson SH. Properties of presynaptic P2X(7)-like receptors at the neuromuscular junction. Brain Res 2005;1034:40–50.
[23] Ireland MF, Noakes PG, Bellingham MC. P2X7-like receptor subunits enhance excitatory synaptic transmission at central synapses by presynaptic mechanisms. Neuroscience 2004;128:269–80.
[24] García-Lecea M, Sen RP, Soto F, Miras-Portugal MT, Castro E. P2 receptors in cerebellar neurons: molecular diversity of ionotropic ATP receptors in Purkinje cells. Drug Dev Res 2001;52:104–13.
[25] Hervás C, Pérez-Sen R, Miras-Portugal MT. Co-expression of functional P2X and P2Y nucleotide receptors in single cerebellar granule cells. J Neurosci Res 2003;73:384–99.
[26] Hervás C. Receptores de nucleótidos en neuronas granulares de cerebelo de rata. Tipos y señalización. Tesis Doctoral. Universidad Complutense de Madrid; 2004.
[27] Sim JA, Young MT, Sung HY, North RA, Surprenant A. Reanalysis of P2X7 receptor expression in rodent brain. J Neurosci 2004;24:6307–14.
[28] Dunkley PR, Jarvie PE, Heath JW, Kidd GJ, Rostas JA. A rapid method for isolation of synaptosomes on Percoll gradients. Brain Res 1986;372:115–29.
[29] Grynkiewicz G, Poenie M, Tsien RY. A new generation of $Ca^{2+}$ indicators with greatly improved fluorescence properties. J Biol Chem 1985;260:3440–50.
[30] Pintor J, Gualix J, Miras-Portugal MT. Diinosine polyphosphates, a group of dinucleotides with antagonistic effects on diadenosine polyphosphate receptor. Mol Pharmacol 1996;51:277–84.
[31] Díaz-Hernandez M, Gómez-Villafuertes R, Hernando F, Pintor J, Miras-Portugal MT. Presence of different ATP receptors on rat midbrain single synaptic terminals. Involvement of the P2X(3) subunits. Neurosci Lett 2001;301(3):159–62.
[32] Herzog E, Bellenchi GC, Gras C, Bernard V, Ravassard P, Bedet C, et al. The existence of a second vesicular glutamate transporter specifies subpopulations of glutamatergic neurons. J Neurosci 2001;21:RC181.
[33] Varoqui H, Schafer MK, Zhu H, Weihe E, Erickson JD. Identification of the differentiation-associated $Na^+$/PI transporter as a novel vesicular glutamate transporter expressed in a distinct set of glutamatergic synapses. J Neurosci 2002;22:142–55.

[34] Loesch A, Burnstock G. Electron-immunocytochemical localization of $P2X_1$ receptors in the rat cerebellum. Cell Tissue Res 1998;294: 253–60.
[35] Gu JG, Heft MW. P2X receptor mediated purinergic sensory pathways to the spinal cord dorsal horn. Purinergic Signall 2004;1: 11–6.
[36] Lewis C, Neidhart S, Holy C, North RA, Buell G, Surprenant A. Coexpression of P2X2 and P2X3 receptor subunits can account for ATP-gated currents in sensory neurons. Nature 1995;377:432–5.
[37] Labrakakis C, Tong CK, Weissman T, Torsney C, MacDermott AB. Localization and function of ATP and GABAA receptors expressed by nociceptors and other postnatal sensory neurons in rat. J Physiol 2003;549:131–42.
[38] Tsuda M, Koizumi S, Kita A, Shigemoto Y, Ueno S, Inoue K. Mechanical allodynia caused by intraplantar injection of P2X receptor agonist in rats: involvement of heteromeric P2X2/3 receptor signaling in capsaicin-insensitive primary afferent neurons. J Neurosci 2000;20: RC90.
[39] Jiang LH, Kim M, Spelta V, Bo X, Surprenant A, North RA. Subunit arrangement in P2X receptors. J Neurosci 2003;23:8903–10.
[40] Gómez-Villafuertes R, Pintor J, Gualix J, Miras-Portugal MT. $GABA_B$ receptor-mediated presynaptic potentiation of ATP ionotropic receptors in rat midbrain synaptosomes. Neuropharmacology 2003;44:311–23.
[41] Virginio C, Church D, North RA, Surprenant A. Effects of divalent cations, protons and calmidazolium at the rat $P2X_7$ receptor. Neuropharmacology 1997;36:1285–94.
[42] King BF, Townsend-Nicholson A. Nucleoside and nucleotide receptors. Tocris Rev 2003;23:1–11.
[43] Jiang LH, Mackenzie AB, North RA, Surprenant A. Brilliant Blue G selectively blocks ATP-gated rat P2X(7) receptors. Mol Pharmacol 2000;58:82–8.
[44] Hibell AD, Thompson KM, Xing M, Humphrey PP. Michel AD Complexities of measuring antagonist potency at P2X(7) receptor orthologs. J Pharmacol Exp Ther 2001;296:947–57.
[45] Allgaier C, Reinhardt R, Schadlich H, Rubini P, Bauer S, Reichenbach A, et al. Somatic and axonal effects of ATP via $P2X_2$ but not $P2X_7$ receptors in rat thoracolumbar sympathetic neurones. J Neurochem 2004;90:359–67.
[46] Atkinson L, Batten TF, Moores TS, Varoqui H, Erickson JD, Deuchars J. Differential co-localisation of the P2X7 receptor subunit with vesicular glutamate transporters VGLUT1 and VGLUT2 in rat CNS. Neuroscience 2004;123:761–8.
[47] Le Feuvre RA, Brough D, Touzani O, Rothwell NJ. Role of P2X7 receptors in ischemic and excitotoxic brain injury in vivo. J Cereb Blood Flow Metab 2003;23:381–4.
[48] Doble A. The role of excitotoxicity in neurodegenerative disease: implications for therapy. Pharmacol Ther 1999;81:163–221.
[49] Neary JT, Kang Y, Willoughby KA, Ellis EF. Activation of extracellular signal-regulated kinase by stretch-induced injury in astrocytes involves extracellular ATP and P2 purinergic receptors. J Neurosci 2003;23:2348–56.
[50] Merlo D, Volonte C. Binding and functions of extracellular ATP in cultured cerebellar granule neurons. Biochem Biophys Res Commun 1996;225:907–14.
[51] Khakh BS, Zhou X, Sydes J, Galligan JJ, Lester HA. State-dependent cross-inhibition between transmitter-gated cation channels. Nature 2000;406:405–10.
[52] Díaz-Hernández M, Sánchez-Nogueiro J, Pintor J, Miras-Portugal MT. Interaction between dinucleotide and nicotinic receptors in individual cholinergic terminals. J Pharmacol Exp Ther 2004;311.
[53] Sokolova E, Nistri A, Giniatullin R. Negative cross-talk between anionic GABAA and cationic P2X ionotropic receptors of rat dorsal root ganglion neurons. J Neurosci 2001;21:4958–68.